Membranes with Fluctuating Topology: Monte Carlo Simulations

G. Gompper[1] and D. M. Kroll[2]
[1]*Max-Planck-Institut für Kolloid- und Grenzflächenforschung, Kantstrasse 55, 14513 Teltow, Germany*
[2]*Department of Medicinal Chemistry and Minnesota Supercomputer Institute, University of Minnesota, 308 Harvard Street SE, Minneapolis, Minnesota 55455*
(Received 29 May 1998)

Much of the phase behavior observed in self-assembling amphiphilic systems can be understood in the context of ensembles of random surfaces. In this article, it is shown that Monte Carlo simulations of dynamically triangulated surfaces of fluctuating topology can be used to determine the structure and thermal behavior of sponge phases, as well as the sponge-to-lamellar transition in these systems. The effect of the saddle-splay modulus, $\bar{\kappa}$, on the phase behavior is studied systematically for the first time. Our data provide strong evidence for a positive logarithmic renormalization of $\bar{\kappa}$; this result is consistent with the lamellar-to-sponge transition observed in experiments for decreasing amphiphile concentration. [S0031-9007(98)07097-5]

PACS numbers: 64.70.–p, 68.10.–m, 82.70.–y

Since Scriven's pioneering suggestion [1] more than twenty years ago that microemulsions are bicontinuous structures, there has been considerable progress in understanding the structure and phase behavior of dilute amphiphilic mixtures [2]. In particular, the bicontinuous structure of microemulsions has been confirmed [3,4], the scattering intensity in both bulk [5] and film contrast [6] has been analyzed, and the similarities with sponge phases have been emphasized [7]. These studies have led to the generally accepted picture that microemulsions in ternary systems containing oil, water, and long-chain amphiphiles consist of two multiply connected networks of oil and water channels which are separated by an amphiphilic monolayer. Similarly, the sponge phase in binary mixtures consists of an amphiphilic bilayer which separates two disconnected water networks.

In the long-chain limit, the molecular solubility of amphiphiles in oil and water is extremely low, and essentially all amphiphiles are contained in supramolecular aggregates consisting of extended, nearly incompressible, two-dimensional monolayer or bilayer membranes [8]. These surfaces can be described as an ensemble of fluctuating surfaces whose shapes and fluctuation spectra are determined by the continuum elastic energy [9]

$$\mathcal{H} = \int dS \left[\frac{\kappa}{2} (c_1 + c_2 - 2c_0)^2 + \bar{\kappa} c_1 c_2 \right], \quad (1)$$

where the integral is taken over the area of the membrane. Here, κ is the bending rigidity, $\bar{\kappa}$ is the saddle-splay modulus, c_0 is the spontaneous curvature, and $c_i = 1/R_i$, with the principal radii of curvature R_1 and R_2. The spontaneous curvature vanishes in binary systems due to the symmetry of the bilayer; in ternary systems, it is zero for special choices of control parameters such as the temperature or salt concentration. We will assume that $c_0 = 0$ throughout this paper.

A theoretical analysis of this model is very difficult. Various approximations have therefore been used to obtain predictions for the structure and phase behavior of these systems. In Refs. [10,11], the role of membrane undulations, which lead to a scale-dependent reduction of the bending rigidity κ [12], has been emphasized. The influence of $\bar{\kappa}$ on the phase behavior is difficult to incorporate in this approach, and it is generally ignored. On the other hand, the importance of the saddle-splay modulus in promoting the irregular, bicontinuous structure of a microemulsion or sponge phase was stressed in Ref. [13]. In fact, it has become increasingly clear recently that *both* effects have to be taken into account in order to understand the lamellar-to-sponge transition [14–16]. This can be seen by rewriting Eq. (1)—for $c_0 = 0$—in the form

$$\mathcal{H} = \int dS \left[\frac{\kappa_+}{2} (c_1 + c_2)^2 + \frac{\kappa_-}{2} (c_1 - c_2)^2 \right], \quad (2)$$

with $\kappa_+ = \kappa + \bar{\kappa}/2$ and $\kappa_- = -\bar{\kappa}/2$. The lamellar phase is energetically stable only if both κ_+ and κ_- are positive. For $\kappa_- < 0$, the flat phase is unstable to the formation of infinite minimal surfaces—or sponge phases. For $\kappa_+ < 0$, there is an instability to a vesicle phase. The effects of thermal fluctuations are incorporated [14] by replacing the elastic moduli in (2) by their renormalized, scale-dependent values, where, to first order in T/κ [12,17],

$$\kappa_\pm(\xi) = \kappa_\pm - \frac{\alpha_\pm T}{4\pi} \ln(\xi/a) \quad (3)$$

with $\alpha_+ = 4/3$ and $\alpha_- = 5/3$. In Eq. (3), a is a microscopic length scale and ξ is a characteristic structural length which is related to the amphiphile volume fraction $\phi = \langle aS/V \rangle$ by $\phi \sim a/\xi$, where S is the membrane area and V is the volume. The lamellar-to-sponge instability is therefore predicted to occur when

$$\ln(\phi/\phi_0) = \frac{2\pi}{\alpha_-} (-\bar{\kappa}/T) \quad (4)$$

 0031-9007/98/81(11)/2284(4)$15.00

with $\bar{\kappa} < 0$, where ϕ_0 is a constant of order unity. It should be emphasized that, although these arguments help explain the phase behavior of these systems, they provide little insight into the structure of the sponge phase itself, e.g., the topology of its multiconnected membrane.

In this paper we report the results of the first systematic Monte Carlo simulation study of the phase behavior of fluid membranes of fluctuating topology in which the fluctuations are controlled by the curvature energy (1). In our model, the membranes are described using the same dynamically triangulated networks which have been employed in simulation studies of the thermal behavior of fluid membranes of fixed topology [18,19]. The membranes consist of a triangular network of beads of diameter a_0 which are linked by flexible tethers of maximum extension ℓ_0. In order to allow the topology to change, a new kind of Monte Carlo step—in addition to bead moves and bond flips—has been introduced. When two different membrane segments—which may or may not be part of the same membrane—come in close spatial proximity, an attempt is made to create a "minimal" neck (or passage) by first removing a surface triangle from each membrane segment and then inserting six new surface triangles which form a tubular connection between the holes in each segment. Similarly, whenever a minimal neck is present, an attempt is made to remove six surface triangles in the neck. Special care has to be taken to guarantee detailed balance [20]. Our procedure for topology change implies that the number N of vertices remains constant during the simulation, but the number N_b of tethers (or bonds) and the number N_t of triangles changes. Periodic boundary conditions are used in a cubic simulation box.

In order to avoid problems with two-phase coexistence regions, we employ a constant pressure ensemble. This has the additional advantage in that we have direct access to the equation of state, since we can determine the amphiphile volume fraction as a function of the external pressure. Finally, the curvature energy (1) has to be discretized on the triangulated surface. For the first, mean-curvature-squared contribution, we use the discretized Laplacian

$$\kappa \int dS(c_1 + c_2)^2 \longrightarrow \tau \sum_i \sigma_i (\Delta \mathbf{R})_i^2 , \qquad (5)$$

where $\mathbf{R}_i$ is the position vector of vertex i, and σ_i is its effective area, as described in detail in Ref. [21]. The bending rigidity κ of the continuum model has been determined as a function of τ [21]. One finds $\kappa = \tau$ for $\tau/T \gg 1$, but $\kappa \simeq \tau/2$ in the low-τ regime studied here. More precisely, $\kappa/T = 1.0$ for $\tau/T = 2.0$, and $\kappa/T = 1.7$ for $\tau/T = 3.0$, with an uncertainty of about 20%. For the second, Gaussian curvature contribution, the Gauß-Bonnet theorem implies

$$\frac{1}{2\pi} \int dS\, c_1 c_2 = \chi_E = N - N_b + N_t \qquad (6)$$

in the case of periodic boundary conditions, where χ_E is the Euler characteristic, which is twice the number of disjunct membrane components minus the number of handles.

The Euler characteristic χ_E characterizes the internal structure of amphiphilic mesophases. For an ideal lamellar phase without defects, $\chi_E = 0$, while for a sponge and vesicle phase, $\chi_E \ll 0$ and $\chi_E \gg 0$, respectively. In fact, the Euler characteristic itself is not a good measure for the connectivity of a sponge phase, since it is an *extensive* quantity. We therefore use the scaled Euler characteristic [22]

$$\gamma \equiv -\langle \chi_E V^2 S^{-3} \rangle . \qquad (7)$$

Our results for the equation of state in the sponge phase for $\kappa/T = 1.0$ and various values of $\bar{\kappa}$ are shown in scaled form in Fig. 1. With decreasing pressure p, the amphiphile volume fraction ϕ first decreases and then saturates at a value which depends on the saddle-splay modulus. This saturation indicates emulsification failure; the sponge phase can no longer be swollen by adding water, but coexists at this point with an almost pure water phase. Figure 1 shows that the Monte Carlo data are very well described by an equation of state of the form

$$pa^3/T \equiv \frac{1}{T}[\phi\, \partial f/\partial \phi - f]$$
$$= [A(\kappa/T, \bar{\kappa}/T) + B(\kappa/T, \bar{\kappa}/T) \ln(\phi)]\phi^3 , \quad (8)$$

where $f(\phi)$ is the free-energy density. It has been argued in Refs. [6,13] that the second equality in Eq. (8) follows from the scale invariance of the curvature energy together

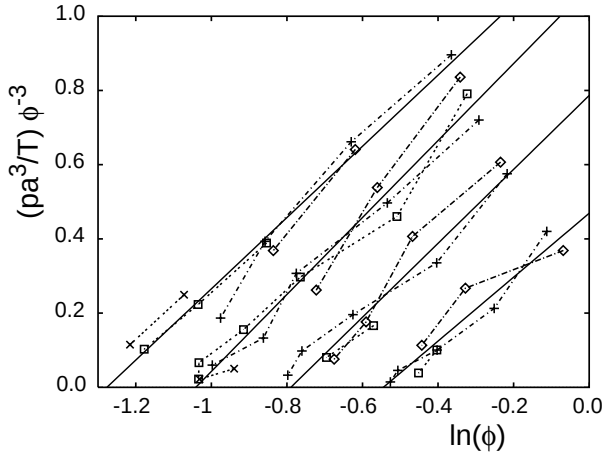

FIG. 1. Equation of state $[p(\phi)a^3/T]\phi^{-3}$ vs $\ln(\phi)$ of sponge phases for $\kappa/T = 1.0$, with $\bar{\kappa}/T = -0.4$, $\bar{\kappa}/T = -0.5$, $\bar{\kappa}/T = -0.6$, and $\bar{\kappa}/T = -0.7$ (from right to left). Data are shown for system sizes $N = 127$ ($\diamond$), $N = 247$ ($+$), $N = 407$ ($\square$) and $N = 607$ ($\times$). The solid lines are the fits to the data discussed in the text. In the analysis of the Monte Carlo data, we identify the microscopic scale a with the bead diameter a_0. The tether length $\ell_0 = 1.633 a_0$ is used in all simulation runs. The volume fraction is averaged over 20 to 100 million Monte Carlo sweeps for each data point.

with the logarithmic renormalization of κ and $\bar{\kappa}$. Some experimental evidence for the validity of this ansatz has already been given in Ref. [13]. However, our simulations provide the first direct demonstration that this relation is correct in the curvature model. Furthermore, the dependence of A and B on the saddle-splay modulus can now be studied systematically for the first time. These functions are intimately related to the structure of a sponge phase; for example, the larger the multiple connectivity of the membrane, the larger is the amplitude of the $\bar{\kappa}$ dependence of A in Eq. (8). A simple linear ansatz for the data presented in Fig. 1 gives $A(\bar{\kappa}/T)/B(\bar{\kappa}/T) = -(a_{11} + a_{12}\bar{\kappa}/T)$, with $a_{11} = 0.44 \pm 0.01$, $a_{12} = 2.46 \pm 0.03$, and $B(\bar{\kappa}/T) = 0.96 \pm 0.03$ for $\kappa/T = 1.0$. Our data for $\kappa/T = 1.7$ are considerably less reliable, since the relaxation times are longer and the finite size effects are more pronounced in a system with larger bending rigidity. In this case, least-squared fits to the data are consistent with $A(\bar{\kappa}/T)/B(\bar{\kappa}/T) = -(a_{21} + a_{22}\bar{\kappa}/T)$ with $a_{21} = 0.59 \pm 0.06$, $a_{22} = 2.71 \pm 0.11$, and $B(\bar{\kappa}/T) = 0.90 \pm 0.10$.

The negative sign of the amplitude of the $\bar{\kappa}/T$ term in $A(\bar{\kappa}/T)$ follows directly from Eq. (1) and the negative Euler characteristic of a sponge phase. The fact that $B(\bar{\kappa}/T)$ does not depend on $\bar{\kappa}/T$ for $\kappa/T = 1.0$ seems to indicate that the internal structure of the sponge phase remains unchanged—up to an overall rescaling. However, the structural parameter γ does change; it decreases from $\gamma \simeq 0.17 \pm 0.01$ at $\bar{\kappa}/T = -0.4$ to $\gamma \simeq 0.12 \pm 0.01$ at $\bar{\kappa}/T = -0.7$, where the error estimate includes the weak pressure dependence of γ for fixed $\bar{\kappa}$. A typical configuration in the sponge phase is shown in Fig. 2a.

At sufficiently negative saddle-splay modulus, or at sufficiently large pressure, the system may transform into a lamellar phase. Our data for the sponge-to-lamellar phase boundary for $\kappa/T = 1.7$ are compared with the prediction (4) for the stability limit of the lamellar phase in Fig. 3. The agreement of the slopes is quite remarkable. Our data therefore provide the first confirmation of a positive renormalization of the saddle-splay modulus. Furthermore, we find that the (universal) amplitude $\alpha_- = 5/3$ is in good agreement with our simulation results. However, a factor ϕ_0 much larger than unity is required in Eq. (4) to fit the data; this indicates that the transition to the sponge phase occurs well before the stability limit of the lamellar phase is reached. The positive renormalization of $\bar{\kappa}$ is very important, since it provides a mechanism for the formation of cubic bicontinuous phases with a lattice constant of order of several thousand angstroms [23]. We expect such phases in our model at higher bending rigidities.

Two other forms for the free energy $f(\phi)$ have been suggested recently [24,25]. In both cases, the renormalization of κ and $\bar{\kappa}$ is *not* considered. Although it is difficult to rule out these suggestions on the basis of the functional dependence of the pressure $p(\phi)$—due to the limited range of ϕ values that we are able to simulate—we have found

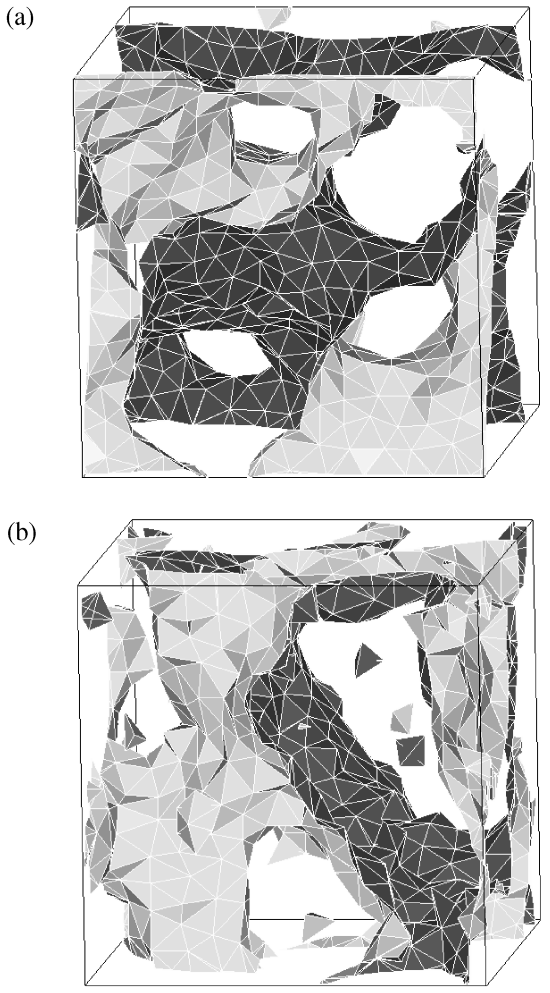

FIG. 2. Typical membrane configurations (for $N = 607$ and $\ell_0 = 1.633a_0$). (a) Sponge phase for $\kappa/T = 1.7$, $\bar{\kappa}/T = -0.7$, and $pa^3/T = 0.001$. (b) Sponge phase for $\kappa/T = 1.0$, $\bar{\kappa}/T = -0.8$, and $pa^3/T = 0.01$. The two sides of the membrane are colored differently to emphasize the bicontinuous structure.

that they do not allow for a consistent interpretation of our simulation data. In Ref. [24], emulsification failure requires a small, positive saddle-splay modulus, while our data show that it occurs for negative $\bar{\kappa}$ (of order $-\kappa$). The Gaussian random-field approach of Ref. [25], on the other hand, predicts emulsification failure at negative $\bar{\kappa}$, but predicts $\phi \sim (2\kappa - 5\bar{\kappa})^{-1/3}$, which is not supported by the data presented in Fig. 3. See Refs. [16,26] for a critical discussion of these models.

For $\kappa/T = 1.0$, the coexistence of the sponge phase with the vesicle phase of very low volume fraction can be seen explicitly for $\bar{\kappa}/T = -0.8$. For $pa^3/T \leq 0.003$, the volume fraction decreases and the Euler characteristic increases roughly linearly with Monte Carlo time in this case. For $pa^3/T = 0.01$, the sponge phase is stable—a typical configuration is shown in Fig. 2b—but contains vesicles embedded in a bicontinuous network. As can be

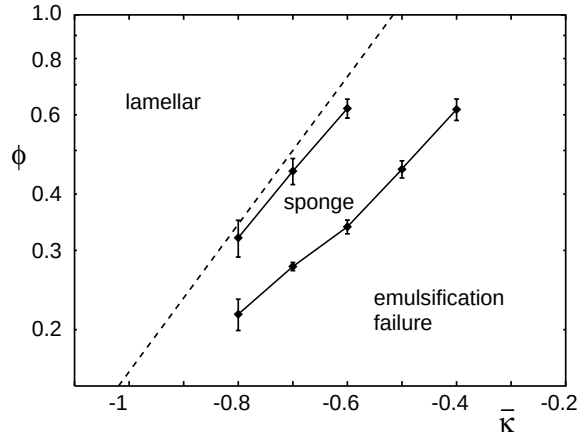

FIG. 3. Phase diagram for $\kappa/T = 1.7$. The upper data set shows the location of the sponge-to-lamellar transition and the lower data set shows the location of emulsification failure. The width of the miscibility gap of the sponge-lamellar coexistence is smaller than the error bars. The approximation (4), with $\phi_0 = 7.0$, for the sponge-to-lamellar transition is shown as a dashed line. Note the logarithmic scale of the ordinate.

seen in Fig. 2b, most of the vesicles have the minimum size of only four beads. This is consistent with recent calculations of the vesicle size distribution, which indicates a maximum at molecular sizes [27]. The phase diagram for $\bar{\kappa}/T \leq -0.9$, where the vesicle phase becomes prominent, remains to be studied in detail. It is important to note that the lamellar phases with an amphiphile volume fraction $\phi < 0.35$ were *not* observed at this value of the bending rigidity (for $\bar{\kappa}/T \geq -0.9$).

We have shown in this paper that Monte Carlo simulations of dynamically triangulated surfaces of fluctuating topology can provide detailed information on the mesoscopic structure and the phase behavior of amphiphilic systems which cannot be easily obtained by other methods. Simulations of this model and its generalizations can be used to study many other problems in which topology changes are important. Examples include the effect of spontaneous curvature on the structure of a sponge phase [28], the formation of passages in lamellar phases [15,29], the fission of vesicles in external force fields, such as hydrodynamic flow, or the effect of embedded polymers on the swelling behavior of a sponge phase.

We acknowledge support from the National Science Foundation under Grants No. DMR-9405824 and No. DMR-9712134, and the donors of The Petroleum Research Fund, administered by the ACS.

[1] L. E. Scriven, Nature (London) **263**, 123 (1976).
[2] G. Gompper and M. Schick, in *Phase Transitions and Critical Phenomena*, edited by C. Domb and J. Lebowitz (Academic Press, London, 1994), Vol. 16, pp. 1–176.
[3] W. Jahn and R. Strey, J. Phys. Chem. **92**, 2294 (1988).
[4] B. Lindman *et al.*, Colloids Surf. **38**, 205 (1989).
[5] M. Teubner and R. Strey, J. Chem. Phys. **87**, 3195 (1987).
[6] D. Roux *et al.*, Europhys. Lett. **11**, 229 (1990).
[7] M. E. Cates *et al.*, Europhys. Lett. **5**, 733 (1988).
[8] In aqueous surfactant solutions, a fraction of the amphiphiles may also be contained in spherical or cylindrical micelles. We assume below that their density is very small.
[9] W. Helfrich, Z. Naturforsch. **28c**, 693 (1973).
[10] D. Andelman, M. E. Cates, D. Roux, and S. A. Safran, J. Chem. Phys. **87**, 7229 (1987).
[11] L. Golubović and T. C. Lubensky, Phys. Rev. A **41**, 4343 (1990).
[12] L. Peliti and S. Leibler, Phys. Rev. Lett. **54**, 1690 (1985).
[13] G. Porte *et al.*, J. Phys. II (France) **1**, 1101 (1991).
[14] D. C. Morse, Phys. Rev. E **50**, R2423 (1994).
[15] L. Golubović, Phys. Rev. E **50**, R2419 (1994).
[16] D. C. Morse, Curr. Opin. Coll. Interface Sci. **2**, 365 (1997).
[17] F. David, in *Statistical Mechanics of Membranes and Surfaces*, edited by D. Nelson, T. Piran, and S. Weinberg (World Scientific, Singapore, 1989), pp. 157–223.
[18] G. Gompper and D. M. Kroll, Curr. Opin. Colloid Interface Sci. **2**, 373 (1997).
[19] G. Gompper and D. M. Kroll, J. Phys. Condens. Matter **9**, 8795 (1997).
[20] Details of the simulation procedure will be described elsewhere.
[21] G. Gompper and D. M. Kroll, J. Phys. I (France) **6**, 1305 (1996).
[22] G. Gompper and M. Kraus, Phys. Rev. E **47**, 4301 (1993). Note that, in a system of constant area and volume, γ is equivalent to the dimensionless Gaussian curvature $\frac{1}{2\pi}\langle K\rangle (V/S)^2$, where $K = c_1 c_2$.
[23] U. Peter, S. König, D. Roux, and A.-M. Bellocq, Phys. Rev. Lett. **76**, 3866 (1996).
[24] J. Daicic *et al.*, J. Phys. II (France) **5**, 199 (1995).
[25] P. Pieruschka and S. A. Safran, Europhys. Lett. **31**, 207 (1995).
[26] D. Roux, F. Nallet, C. Coulon, and M. E. Cates, J. Phys. II (France) **6**, 91 (1996).
[27] D. C. Morse and S. T. Milner, Phys. Rev. E **52**, 5918 (1995).
[28] T. Tlusty, S. A. Safran, R. Menes, and R. Strey, Phys. Rev. Lett. **78**, 2616 (1997).
[29] G. Gompper and J. Goos, J. Phys. II (France) **5**, 621 (1995).